The Egyptian Journal of Remote Sensing and Space Sciences 25 (2022) 579–592

HOSTED BY

Contents lists available at ScienceDirect

The Egyptian Journal of Remote Sensing and Space Sciences

journal homepage: www.sciencedirect.com

Comparison of recently released satellite altimetric gravity models with shipborne gravity over the Red Sea

Mohamed Abdallah [a,b,*], Rasha Abd El Ghany [a], Mostafa Rabah [a], Ahmed Zaki [c]

[a] Department of Civil Engineering, Benha Faculty of Engineering, Benha University, Egypt
[b] Department of Civil Engineering, New Damietta Higher Institute of Engineering and Technology, Damietta, Egypt
[c] Civil Engineering Department, Faculty of Engineering, Delta University for Science and Technology, Gamasa, Egypt

ARTICLE INFO

Article history:
Received 9 December 2021
Revised 25 February 2022
Accepted 29 March 2022
Available online 5 April 2022

Keywords:
Satellite altimetry
Shipborne gravity
Marine gravity
Red Sea

ABSTRACT

Since 2010, a slew of new satellite altimetry missions has started providing gravity data generated from altimetry with worldwide coverage and high quality that rivals shipborne gravity measurements in several areas. As a result, worldwide offshore high-resolution gravity fields have considerably improved. This paper aims to compare two altimetry gravity models i.e. DTU21 and SSv29.1 with shipborne gravity measurements to evaluate their accuracies over the Red Sea. At first, the DTU21 and SSv29.1 altimetry models were compared with the shipborne data at different water depths to evaluate the impact of bathymetry depths on the accuracy. The corresponding results revealed that the DTU21 gravity model gave the best results in the comparison of all shipborne with a standard deviation (s.d.) of 7.37 mGal and a Root Mean Square (RMS) of 8.73 mGal, while the SSv29.1 model achieve an s.d. of 8.50 mGal and an RMS of 8.81 mGal. In water depths less than 1000 m the DTU21 model gives the best results in terms of s.d. and RMS, while the SSv29.1 model achieves better results at water depths ranging between 1000 m and 3000 m.

1. Introduction

The gravity potential is among the most fundamental fields on Earth, reflecting the movement, masses distribution, and state of the changing of the Earth's inner material. Because the water covers around 70% of the Earth's surface, the marine gravity data are significant sources for constructing the gravity field. High-resolution marine gravity measurements are critical for bathymetry estimation, marine geological structure, studying seafloor topography, mineral resource distributions, and petroleum explorations (Sandwell and Smith, 1997; Liu et al., 2016; Li et al., 2021).

The marine gravity field may be computed at different accuracy from several resources, including shipborne (Zaki et al., 2018b), airborne observations (Forsbergbi et al., 2012), satellite gravity missions (Abdallah et al., 2022; Zaki et al., 2018a), and satellite altimetry (Li et al., 2021). Although the accuracy of shipborne and airborne observations make them essential solutions for constructing the worldwide marine gravity field, the marine gravity data measured onboard ships and airborne usually have sparse data coverage, long measurement periods, and a lack of repeated observations, making it impossible to obtain global marine gravity information at a suitable cost and time.

In recent years, satellite altimetric missions have become a very important tool for determining the regional and global marine gravity data by dint of its high resolution and data accessibility (Sandwell et al., 2014). Satellite altimeters have noticeably enhanced the accuracy and spatial resolution of altimetry, ranging from first-generation altimeters such as TOPEX/Poseidon, Envisat, Jason-1, and Jason-2, to the modern generations, such as CryoSat-2, Sentinel-3, Sentinel-6, and SARAL/AltiKa.

Satellite altimetric gravity models, such as DTU21 (Andersen and Knudsen, 2020) and SSv29.1 (Sandwell et al., 2021), are important models for giving information on marine gravity, particularly in regions with limited ship coverage. Near the coast and in shallow water, the precision of altimetric measurements reduces. This is due to poor tidal modeling near coastlines, significant sea surface variation, and the loss of altimeter tracking due to onshore reflector interference.

Peer review under responsibility of National Authority for Remote Sensing and Space Sciences.

* Corresponding author.
E-mail address: e.mohamedabdallah@gmail.com (M. Abdallah).

https://doi.org/10.1016/j.ejrs.2022.03.016
1110-9823/

In this study, the shipborne data A. Zaki et al., (2018b) are used to examine the reliability of altimetric gravity models (DTU21 and SSv29.1) along the Red Sea at various water depths. Section 2 describes the sources of different gravity data used in the study. The comparisons of shipborne gravity measurements with gravity models obtained from satellite altimetry are provided in Section 3.1. The comparisons between the two gravity models relative to each other at various water depths are performed in Section 3.2. Finally, in Section 4, some conclusions are reached.

2. Marine gravity data

2.1. Shipborne gravity data

In this study, the shipborne data are used from Zaki et al., (2018b). In the Red Sea, (Zaki et al., 2018b) filtered shipborne gravity data from the Bureau Gravimétrique International (BGI). Both the cross-validation method and interpolation technique were utilized to guarantee that the shipborne gravity observations are con-

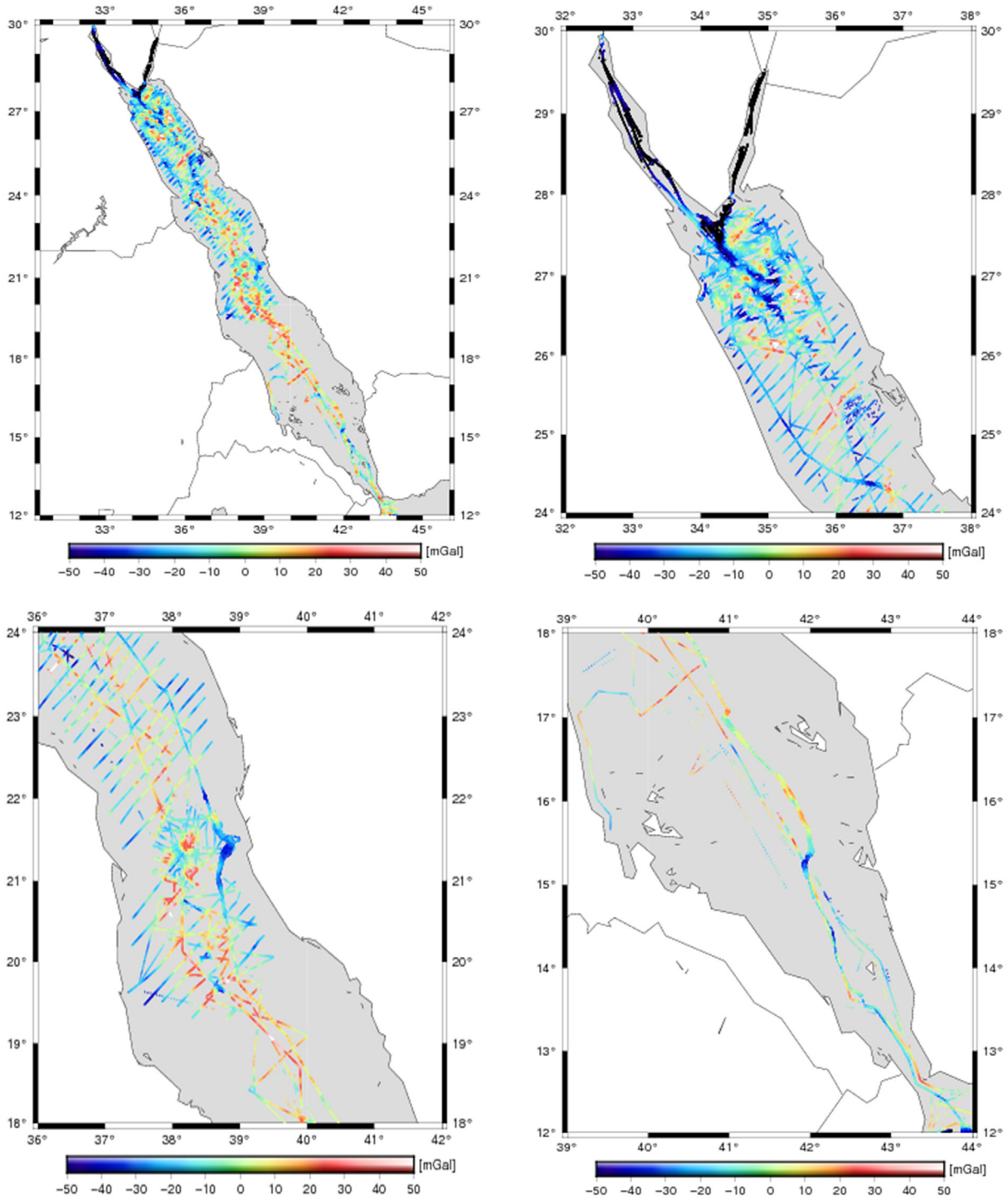

Fig. 1. Free-air anomalies of the Shipborne gravity data along the Red Sea. (For interpretation of the references to colour in this figure legend, the reader is referred to the web version of this article.)

sistent and mistake-free. As seen in Fig. 1, the input shipborne gravity data used for this investigation comprises 75,019 gravity points.

2.2. Altimetric gravity data

The development of satellite altimetry has led to the construction of regional and global marine gravity models by many institutions and research groups, as they have been continuously exploring higher-quality global marine gravity field models and performing achievements from generation to generation.

As shown in Table 1, the Scripps Institution of Oceanography (SIO) released the S&S series of marine gravity models. Since 1997, (Sandwell and Smith, 1997) constructed the global marine gravity field model V7.2. With the acquisition of additional data from satellite altimetry, new reference gravity fields, the emergence of waveform retracking, and improvements in the data processing.

In addition, Sandwell's team has successively published a series of global marine gravity field models. For example, models V18.1 (Sandwell and Smith, 2009) retracked the raw waveforms from the ERS-1 and Geosat/GM missions to improve the range precision and used the EGM2008 global gravity model as a reference field to obtain a smooth gravity transition from land to ocean. In V22.1 (Sandwell et al., 2013), Cryosat-2, Jason-1, and Envisat data are added and used with a low-pass filter whose wavelength depends on the depth and slope corrections. In V29.1, sentinel 3A/B data on a 54-day repeat ground track was added (Li et al., 2021). The SSv29.1 gravity model can be downloaded from: ftp://topex.ucsd.edu/pub/archive/grav/.

Another important global marine gravity field model series is released by the Technical University of Denmark (DTU) as shown in Table 2. Andersen and Knudsen (1997) started to calculate the global marine gravity field using satellite altimetry by contract KMS96 model. Over time, the new models included additional satellite altimetry data and used the EGM2008 as a reference field model to increase the accuracy and precision. For example, the DTU13, DTU15, and DTU17 models were computed with CryoSat-2 data. Moreover, the major improvement of DTU17 over DTU15 is that the computation of DTU17 contained more CryoSat-2 and

Table 1
Characteristics of different SS series models (Li et al., 2021).

Models	Year	Reference gravity field	Data	Resolution (arc-minute)	Coverage range
V7.2	1997	JGM-3	Geosat (ERM/GM) and ERS-1 (ERM/GM) data	2 × 2	72°S ~ 72°N
V8.1	1998	EGM96	Geosat and ERS-1 data	1 × 1	72°S ~ 72°N
V11.1	2004	EGM96	Retracked ERS-1 and Geosat data	1 × 1	72°S ~ 72°N
V16.1	2006	EGM96	Geosat, ERS-1 and T/p data	1 × 1	80.7°S ~ 80.7°N
V18.1	2009	EGM2008 + MDOT	(Geosat, ERS-1 and T/p) data + biharmonic spline interpolation	1 × 1	80.7°S ~ 80.7°N
V20.1	2012	EGM2008 + MDOT	Added Jason-1 and Cryosat-2 and Envisat data	1 × 1	80.7°S ~ 80.7°N
V22.1	2013	EGM2008 + MDOT	(Geosat, ERS-1, Cryosat-2, Jason-1, and Envisat) data + the wavelength of the low-pass filter	1 × 1	85°S ~ 85°N
V23.1	2014	EGM2008 + MDOT	Added all of Jason-1/GM data and 9 months of Cryosat-2 data	1 × 1	85°S ~ 85°N
V24.1	2016	EGM2008 + MDOT	Added 12 months of Cryosat-2 data	1 × 1	85°S ~ 85°N
V25.1	2017	EGM2008 + MDOT	Added 1 year of Cryosat-2/LRM data and more than 2 years of Cryosat-2/SAR data and 1 year of Altika data	1 × 1	85°S ~ 85°N
V26.1	2018	EGM2008 + MDOT	Added half-year of Cryosat-2 data and a half year of Altika data	1 × 1	85°S ~ 85°N
V27.1	2019	EGM2008 + MDOT	Added 1 year of retracked Jason-2 data and 2 months of Altika data	1 × 1	85°S ~ 85°N
V28.1	2019	EGM2008 + MDOT	Added more Cryosat-2 and Jason-2 and Altika data + the grid is converted to Cartesian coordinates and stored as NETCDF	1 × 1	85°S ~ 85°N
V29.1	2019	EGM2008 + MDOT	Added 2 years of sentinel-3A/B data	1 × 1	85°S ~ 85°N

Table 2
characteristics of DTU series models (Li et al., 2021).

Models	Year	Reference gravity field	Data	Resolution (arc-minute)	Coverage range
KMS96	1996	EGM96	ERS-1 and Geosat data	3.75 × 3.75	82°S ~ 82°N
KMS02	2002	EGM96	ERS-1, ERS-2 and Geosat data	2 × 2	82°S ~ 82°N
DNSC08	2008	EGM08 + DOT07A	ERS-1, ERS-2, Geosat, T/P, GFO, Jason-1, and ICESat data	1 × 1	90°S ~ 90°N
DTU10	2010	EGM08 + MDOT	Added Envisat data	1 × 1	90°S ~ 90°N
DTU13	2013	EGM08 + MDOT	Added Cryosat-2 data	1 × 1	90°S ~ 90°N
DTU15	2015	EGM08 + MDOT	Retracked ERS-1, Geosat, Cryosat-2, and Jason-1 data.	1 × 1	90°S ~ 90°N
DTU17	2017	EGM08 + MDOT	Added 7 years of Cryosat-2 and Jason-1 data and 12 months of Altika data	1 × 1	90°S ~ 90°N
DTU18	2018	EGM08 + MDOT	Added retracked Altika data and other satellite data	1 × 1	90°S ~ 90°N
DTU21	2021	EGM08 + MDOT	Added 5 years of Sentinel-3A data and 3 years of Sentinel-3B and reprocessed Cryosat-2 data (processed with the SAMOSA + Physical retracker) were added.	1 × 1	90°S ~ 90°N

SARAL/AltiKa data from 2016 to 2017 in the geodetic phase, while the improvement of DTU21 over DTU17 is that the former was computed by combining 5 years of Sentinel-3B and reprocessed Cryosat-2 data (Wu et al., 2022). The used DTU 21 gravity model data in this study can be obtained from https://ftp.space.dtu.dk/pub/.

The DTU21 (Andersen and Knudsen, 2020) and SSv29.1 (Sandwell et al., 2021) satellite altimetry-derived gravity datasets were used in the current study. The two models are provided as grids with a 1 arc-minute resolution, where the satellite altimetric gravity data sets provide offshore coverage (Pavlis et al., 2013). The primary distinction between DTU21 and SSv29.1 is the type of estimate algorithm used. The residual Sea Surface Heights (SSH) (Andersen and Knudsen, 2020) are used in DTU21, whilst the residual slopes of the SSH (Sandwell et al., 2013) are used in SSv29.1, which was determined from mathematical differentiation of nearby altimeter data. Furthermore, the use of residual SSH, in particular, is less influenced by the scarce of data on the side of land in near-coastal locations than the use of residual SSH slopes for a given reference gravitational model whose resolution is always

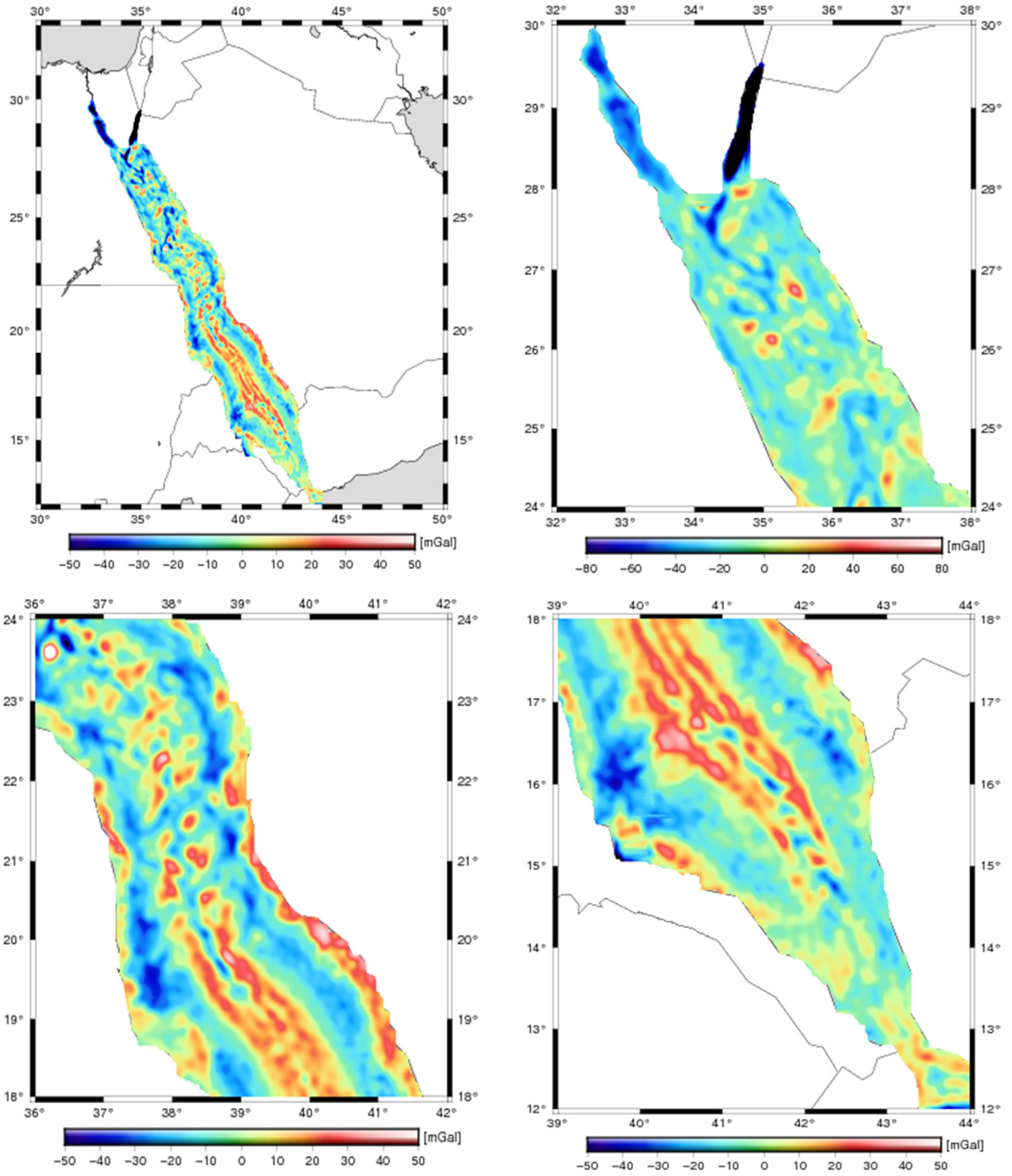

Fig. 2. Free-air gravity anomalies from the DTU21 model along the Red Sea; units [mGal]. (For interpretation of the references to colour in this figure legend, the reader is referred to the web version of this article.)

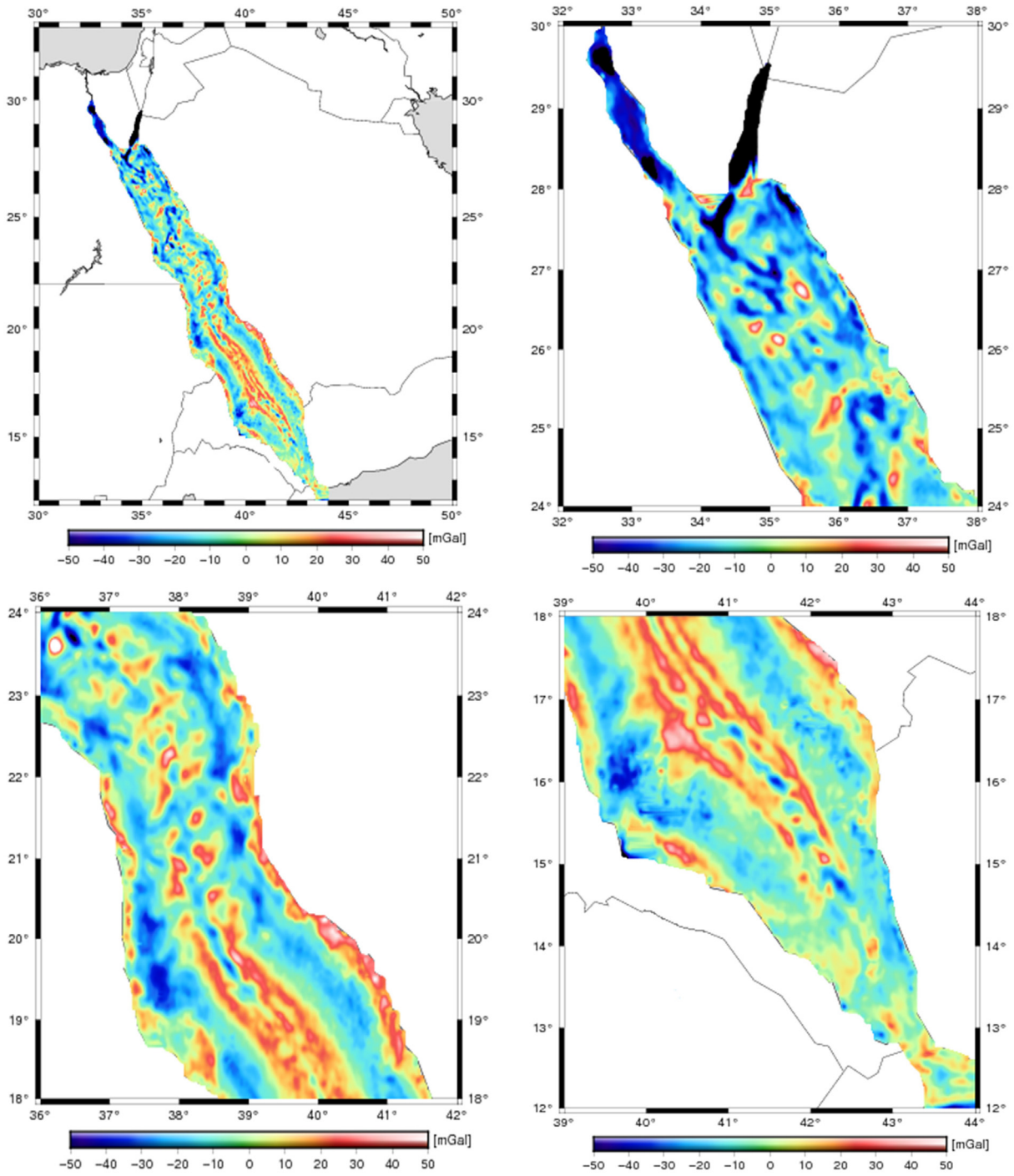

Fig. 3. Free-air gravity anomalies from the SSv29.1 model along the Red Sea; units [mGal]. (For interpretation of the references to colour in this figure legend, the reader is referred to the web version of this article.)

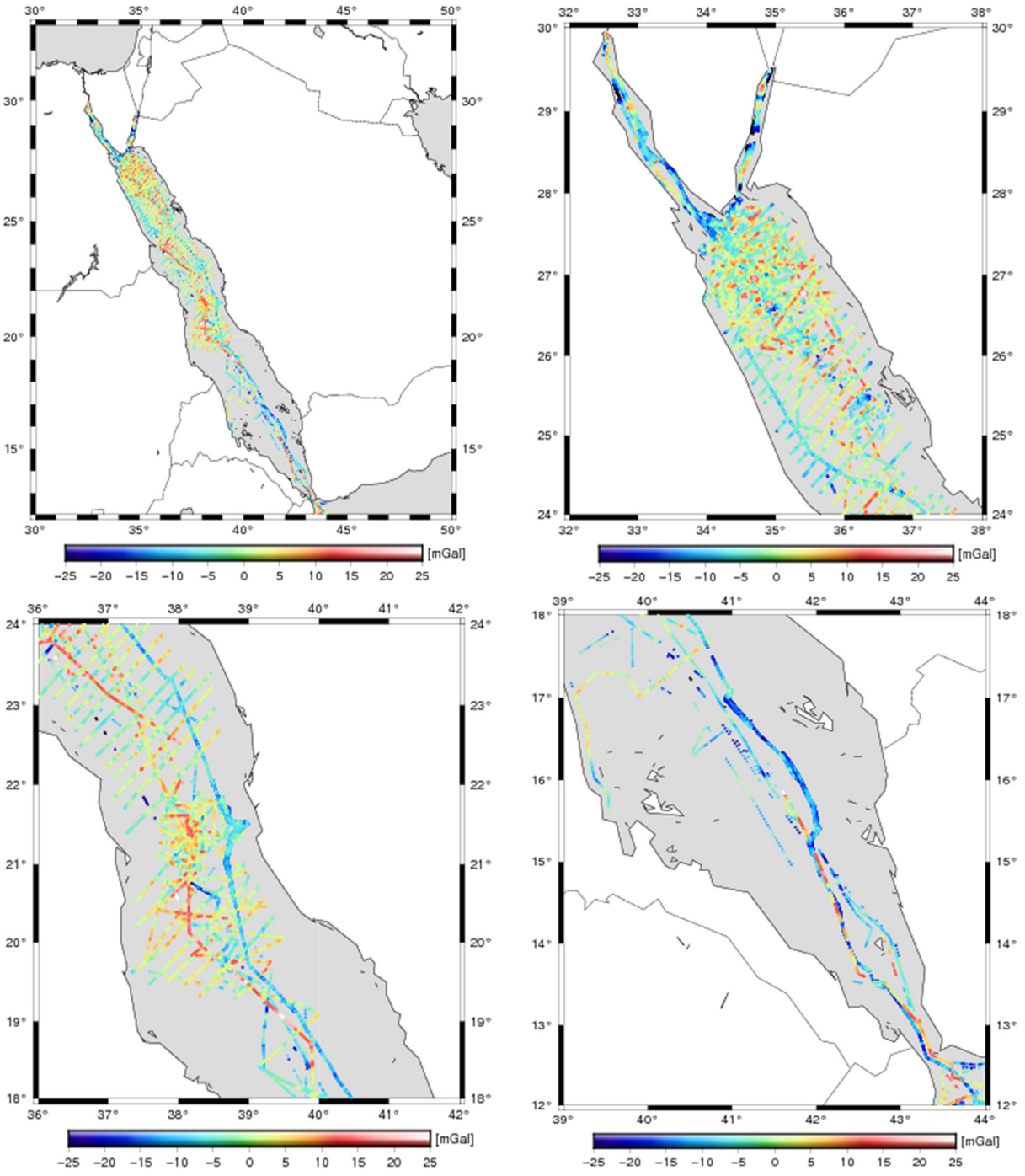

Fig. 4. Difference between the shipborne gravity data and DTU21 model.

finite. In comparison to the usage of residual SSH slopes, residual SSH produces gravity anomalies with more high-frequency content (Pavlis et al., 2013). So, the DTU21 is preferred in near-coastal areas. Fig. 2 shows the free air (FA) gravity values from the DTU21 model, while Fig. 3 shows the free air (FA) gravity values from the SSv29.1 model.

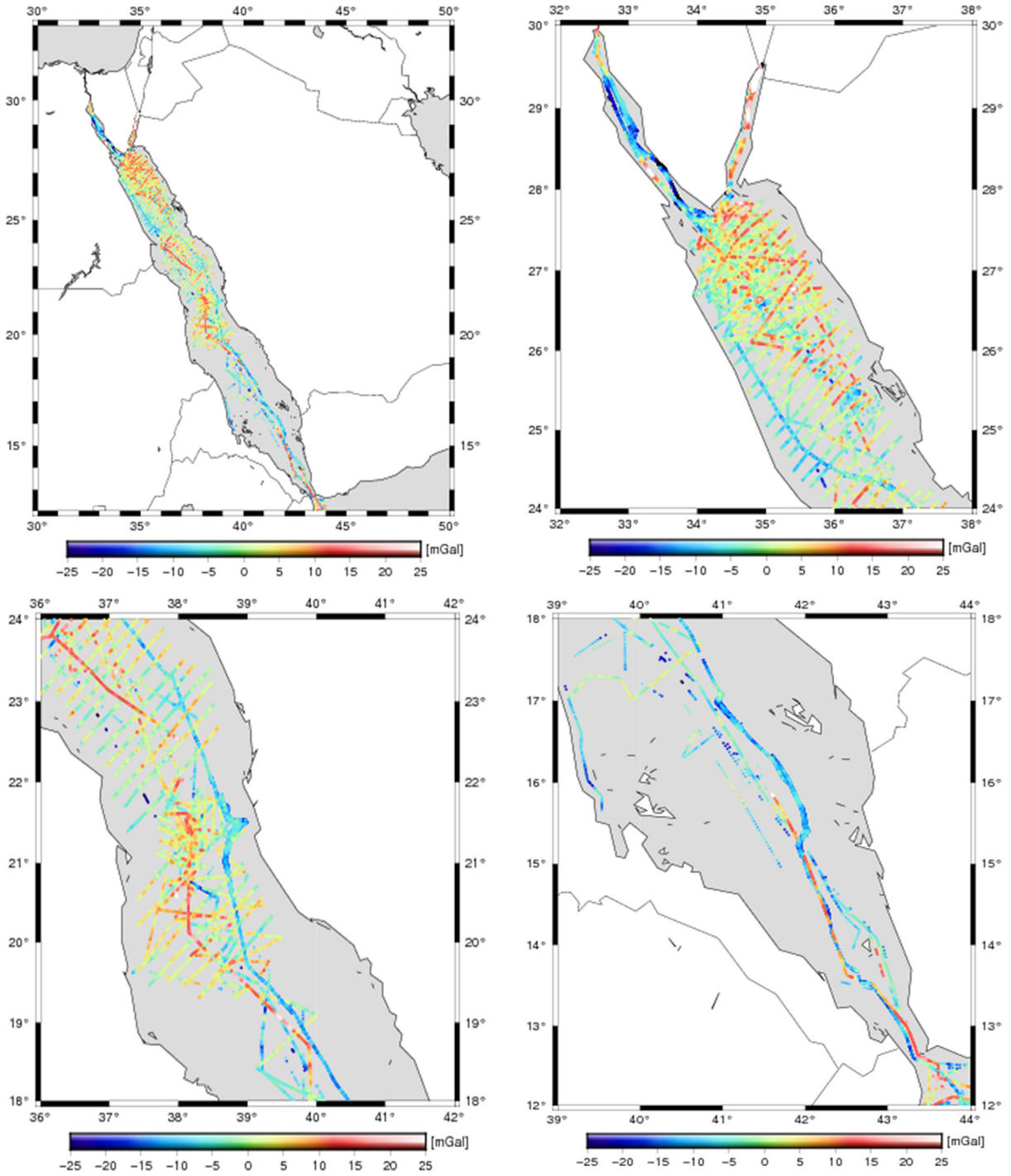

Fig. 5. Difference between the shipborne gravity data and SSv29.1 model.

3. Results and discussion

3.1. Comparison between gravity models derived from satellite altimetry with shipborne gravity data

A. Zaki et al. (2018b) made comparisons between satellite gravity models SSv23.1 and DTU13 with the shipborne gravity data along the Red Sea. They revealed that the s.d. reached 8.71 mGal for the SSv23.1 and 8.83 mGal for the DTU13. The differences between FA gravity data from the DTU21 and SSv29.1 with shipborne gravity data along the Red Sea were calculated and presented in Figs. 4 and 5, respectively. The histogram of the residuals between the DTU21 and SSv29.1 models is shown in Fig. 6. Table 3 summarises the most important statistical results from the difference data statistical analysis. The s.d. of the differences between the DTU21 and SSv29.1 satellite altimetry models and shipborne data in the study area is 7.37 and 8.50 mGal, respectively. For the term of RMS, DTU21 showed the best result with

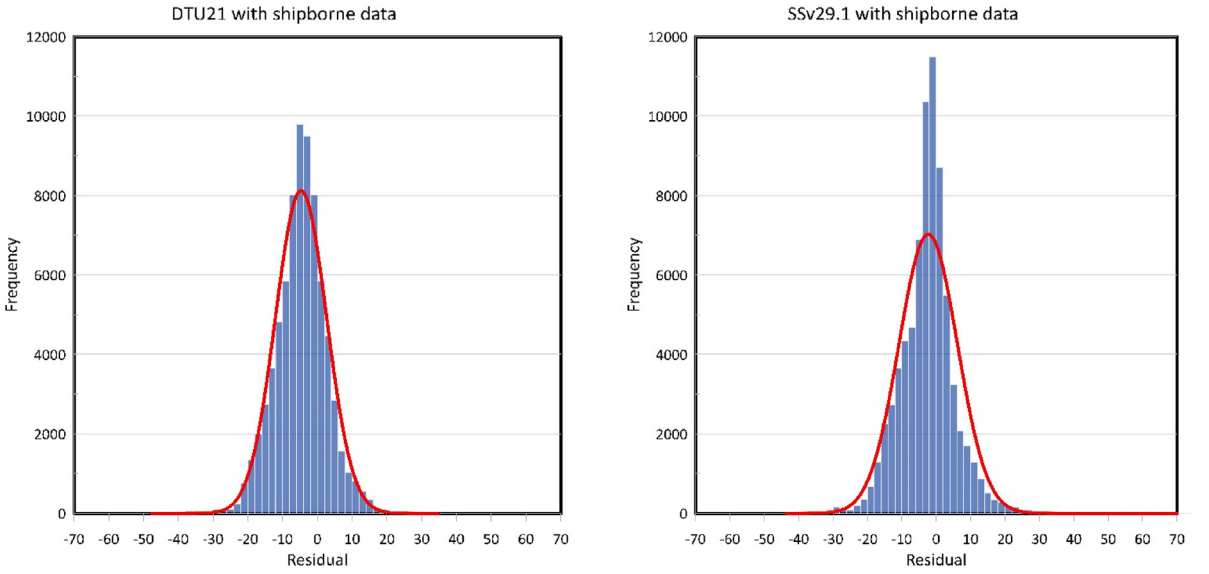

a. Differences between shipborne data and DTU21 model histogram.

b. Differences between shipborne data and SSv29.1 model histogram.

Fig. 6. Differences between shipborne data and (a) DTU21 model, and (b) SSv29.1 model histogram.

Table 3
The difference between shipborne FA gravity data and satellite altimetric FA gravity data from DTU21 and SSv29.1, respectively. units are mGal.

Satellite Gravity Data	Minimum	Maximum	Mean	s.d.	RMS
DTU21– Shipborne gravity	−47.73	34.83	−4.69	7.37	8.73
SSv29.1– Shipborne gravity	−43.56	73.50	−2.32	8.50	8.81

8.73 mGal, while SSv29.1 obtained 8.81 mGal. So it can be concluded that DTU21 showed the best results in the Red Sea.

In shallow water, the accuracy of altimetric gravity is known to decrease. This is because of increased sea surface variation and altimeter tracking loss due to onshore reflector interference. To evaluate the impact of bathymetry depths on the accuracy of altimetric gravity observations, the measurements were grouped into six water-depth ranges, and data analysis of the difference between shipborne gravity data and the altimetry models (DTU21 and SSv29.1) were done for each range. Fig. 7 shows the bathymetry in the Red Sea, as derived from the SRTM15+. Table 4, Figs. 8, and 9 show the statistics of the difference between shipborne gravity data and the gravity data derived from satellite altimetry for each of the water-depth ranges.

For water depths that range between [0 m and 20 m], we see a significant rise in the s.d. and RMS of the difference between shipborne and gravity observations; for DTU21, the s.d. and RMS are 9.17 and 11.54 mGal, respectively, while for SSv29.1, the s.d. and RMS are 10.83 and 12.24 mGal. This is partly due to the fact satellite altimetric gravity is not optimum in coastal regions and complicated areas with islands, because quality decreases near the coast. (Zhang et al., 2017). For water depths that range between [20 m and 1000 m], the DTU21 gravity data generally shows 17.5% less s.d. and 5.7% fewer RMS differences than the SSv29.1, when compared with shipborne data. From the obtained results, for bathymetry depths greater than 1000 m, the s.d. and RMS between the shipborne gravity and the gravity models are a little different in quality, but the SSv29.1 model achieves better performance by 7.3% less s.d. and by 16.8% fewer RMS compared to the DTU21 model.

3.2. Comparison between the two gravity models at various water depths

To investigate the satellite altimetric gravity error, we compare the differences between the DTU21 and the SSv29.1 satellite altimetric gravity models in the Red Sea, at various water depths. Table 5 represents the data of the differences between the DTU21 and SSv29.1 models. The differences are characterized by a minimum, maximum, mean, s.d., and RMS of −46.60, 103.14, 0.68, 4.95, and 4.99 mGal, respectively. Fig. 10 shows the differences between the satellite altimetry gravity values provided by the DTU21 and SSv29.1 models over the Red Sea.

Fig. 11 presents the discrepancies between the satellite altimetric gravity data provided by DTU21 and SSv29.1 models for each of the water-depth intervals. The statistics of the differences between DTU21 and SSv29.1 gravity models along the Red Sea are reported in Table 6, Figs. 12, and 13. From the results, the s.d. and RMS between DTU21 and SSv29.1 models over the Red Sea decrease at high water depths because the quality of altimetric models

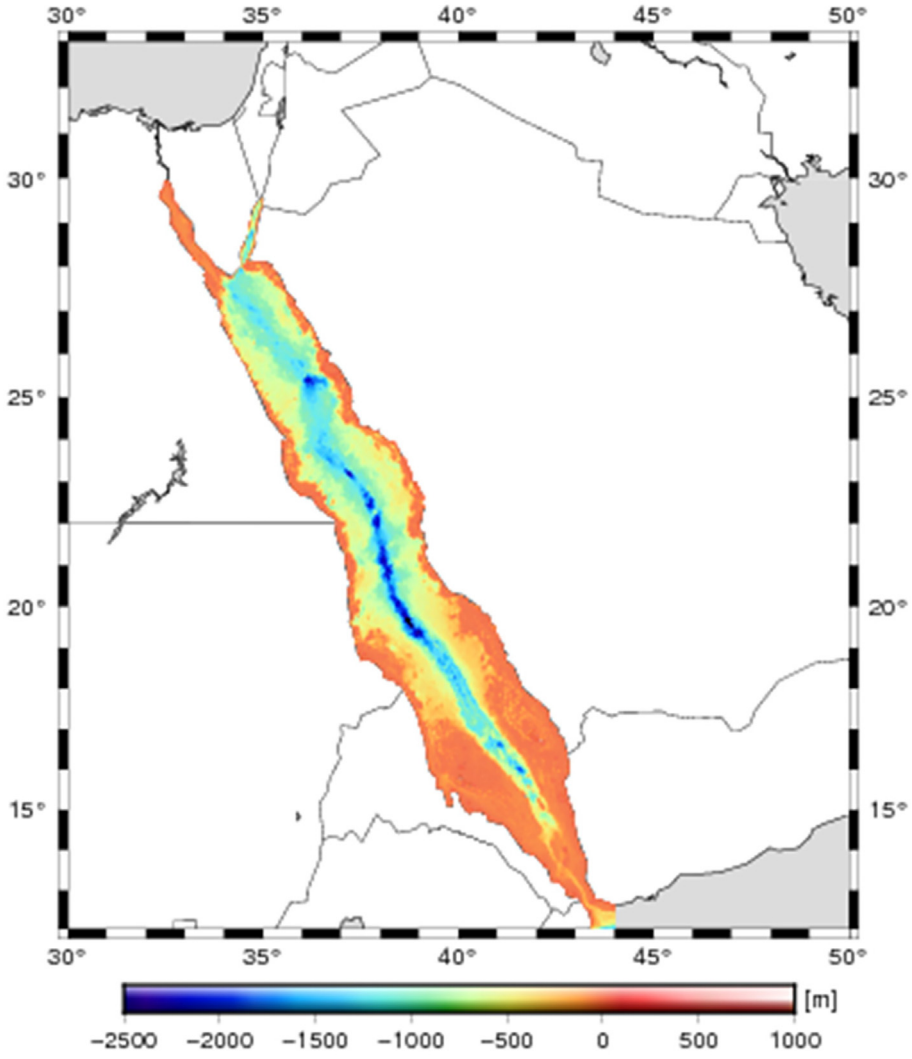

Fig. 7. The bathymetry derived from SRTM15 + over the Red Sea. (For interpretation of the references to colour in this figure legend, the reader is referred to the web version of this article.)

Table 4
The statistics of the differences between the FA gravity from satellite altimetric models and the shipborne FA gravity data; unit [mGal].

Satellite Altimetric Model	Water Depth	Minimum	Maximum	Mean	s.d.	RMS
DTU21	0–20	−25.73	12.59	−7.06	9.17	11.54
	20–50	−23.82	15.75	−6.94	8.58	11.04
	50–100	−32.61	16.09	−8.93	7.49	10.95
	100–1000	−47.73	34.83	−4.66	7.41	8.76
	1000–2000	−22.63	20.81	−4.07	6.99	8.09
	2000–3000	−22.81	16.00	−2.28	5.64	6.08
SSv29.1	0–20	−30.52	16.98	−3.26	10.83	12.24
	20–50	−31.92	23.16	−6.64	10.03	12.03
	50–100	−42.22	34.10	−13.22	9.58	11.54
	100–1000	−43.56	73.50	−2.07	8.80	9.03
	1000–2000	−23.68	33.87	−0.90	6.26	6.32
	2000–3000	−19.07	14.98	−0.55	5.44	5.47

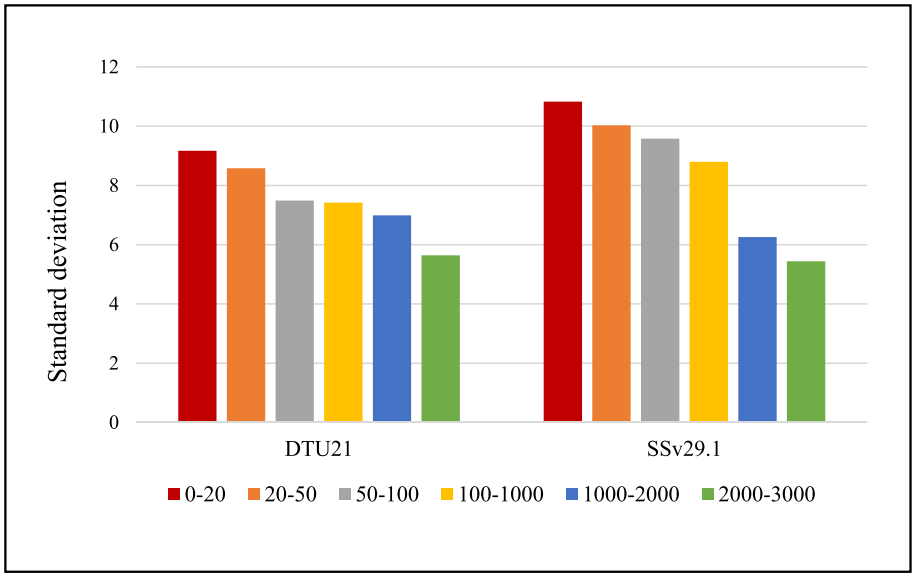

Fig. 8. The s.d. of the differences between the shipborne gravity data, DTU 21 and the SSv29.1 models as a function of bathymetry depths.

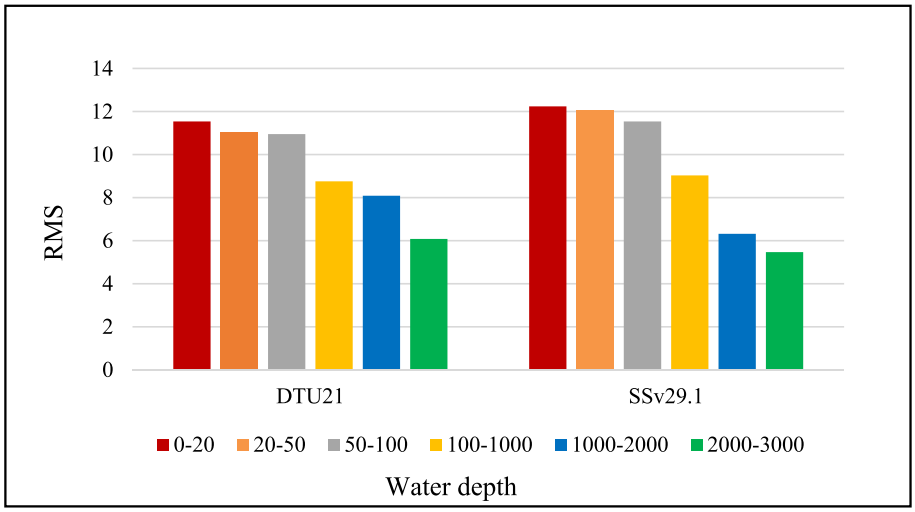

Fig. 9. The RMS of the differences between the shipborne gravity data, DTU 21 and the SSv29.1 models as a function of bathymetry depths.

Table 5
The statistics of the differences between DTU21 and SSv29.1 models; unit [mGal].

Model	Minimum	Maximum	Mean	s.d.	RMS
SSv29.1 – DTU21	−46.60	103.14	0.68	4.95	4.99

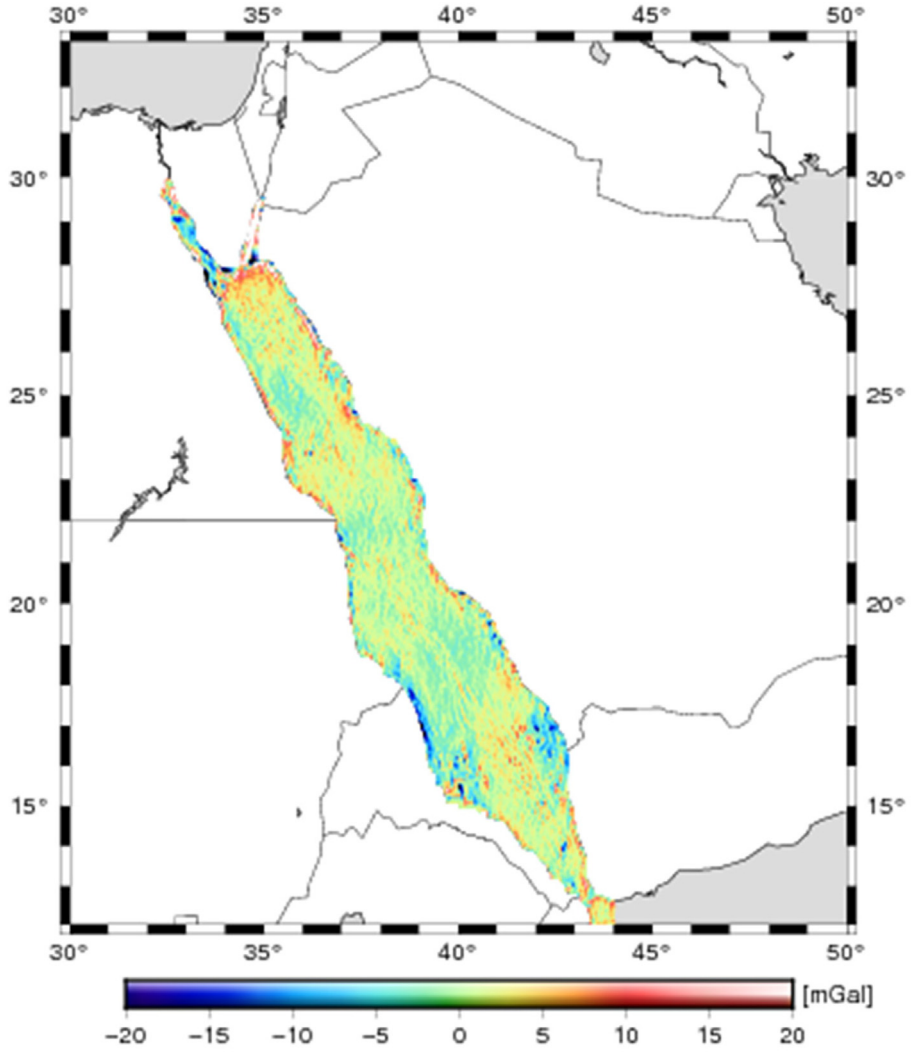

Fig. 10. The differences between FA gravity using DTU21 and SSv29.1 models along the Red Sea: unit [mGal]. (For interpretation of the references to colour in this figure legend, the reader is referred to the web version of this article.)

decreases near the coast. The differences at a water depth range between (0 m and 20 m) are characterized with a minimum, maximum, mean, and s.d. of −46.60, 61.55, −0.11, and 5.83 mGal, respectively. On the other hand, the differences at a water depth range between (2000 m and 3000 m) achieve the best results with a minimum, maximum, mean, s.d., and RMS of −2.18, 7.27, 2.21, 1.71, and 2.79 mGal, respectively.

4. Conclusion

This paper aims to validate the recently released satellite altimetric models such as DTU21 and SSv29.1 gravity data models with shipborne gravity data to evaluate accuracies along the Red Sea. At first, the comparisons between the DTU21 and SSv29.1 with shipborne gravity data are applied and the results demonstrated that the performance of the DTU21 model is better than the SSv29.1 with an s.d. of 7.37 mGal and an RMS of 8.73 mGal. Then, the comparisons between shipborne gravity data with satellite altimetry at various bathymetry depths, data were grouped into six water-depth ranges. The results reveal that the assessed gravity models are not reliable in bathymetry depths less than 20 m due to increased sea surface variability, and failure of altimeter tracking caused by onshore reflector interference. In bathymetry depths range between 20 m and 1000 m, the DTU21 gravity data generally exhibit a 17.5% less s.d. difference than the SSv29.1, when compared with the shipborne data. In bathymetry depths more than 1000 m, the SSv29.1 model achieves better performance in an s.d. by 7.3% less compared to the DTU21 model. Finally, the differences between the DTU21 and SSv29.1 models for each of the

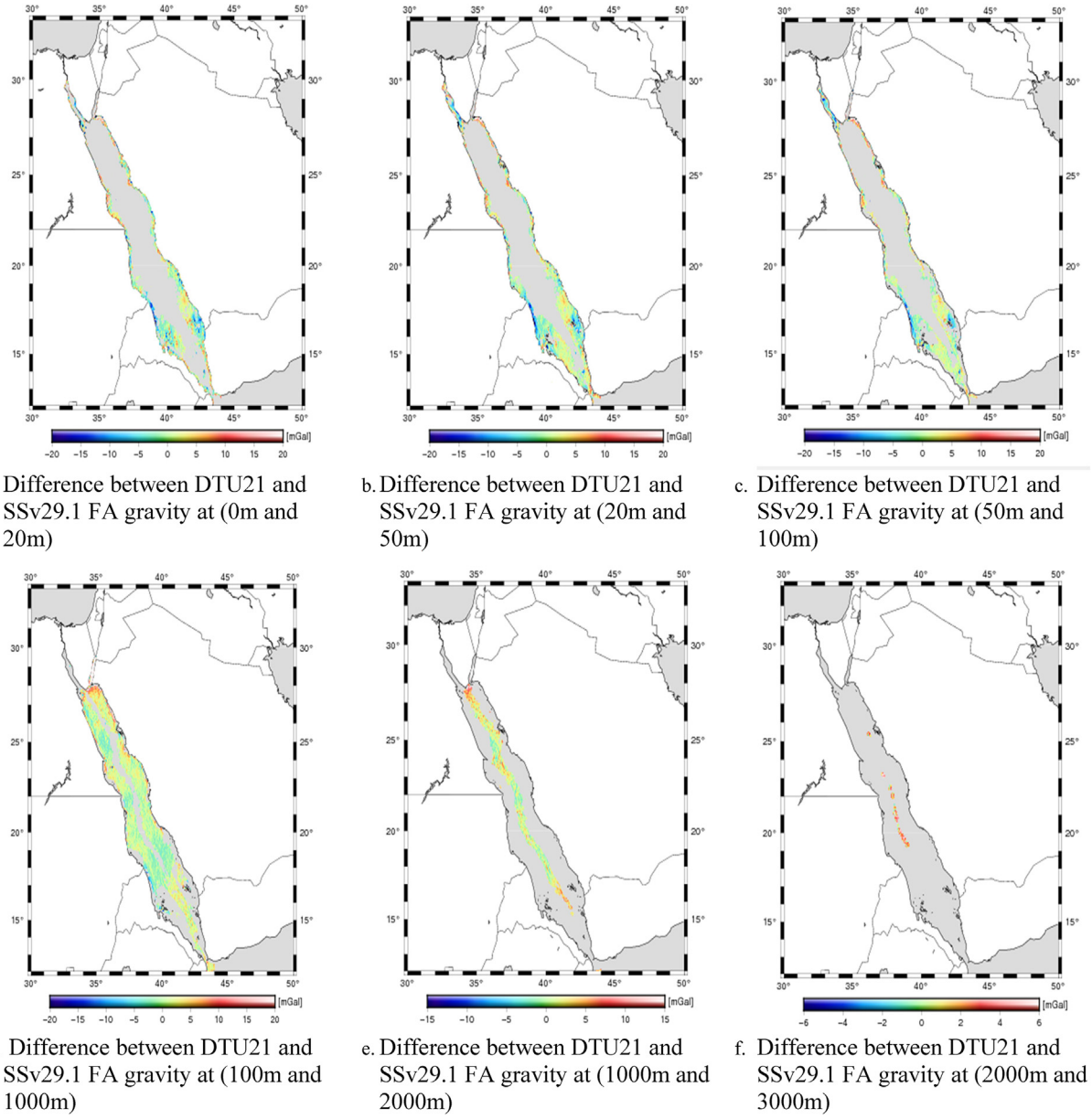

a. Difference between DTU21 and SSv29.1 FA gravity at (0m and 20m)

b. Difference between DTU21 and SSv29.1 FA gravity at (20m and 50m)

c. Difference between DTU21 and SSv29.1 FA gravity at (50m and 100m)

d. Difference between DTU21 and SSv29.1 FA gravity at (100m and 1000m)

e. Difference between DTU21 and SSv29.1 FA gravity at (1000m and 2000m)

f. Difference between DTU21 and SSv29.1 FA gravity at (2000m and 3000m)

Fig. 11. The difference between DTU21 and SSv29.1 FA gravity at various water depths.

Table 6
The characteristics of the differences between the DTU21 and SSv29.1 models at various water depths; unit [mGal].

	At water Depth	Minimum	Maximum	Mean	s.d.	RMS
Difference between SSv29.1 and DTU21 gravity models related to water depth						
	0–20	−46.60	61.55	−0.11	5.83	5.83
	20–50	−45.29	63.56	0.12	5.31	5.31
	50–100	−44.20	63.73	0.36	5.06	5.08
	100–1000	−43.43	102.12	1.02	4.56	4.67
	1000–2000	−7.30	55.02	1.70	3.78	4.14
	2000–3000	−2.18	7.27	2.21	1.71	2.79

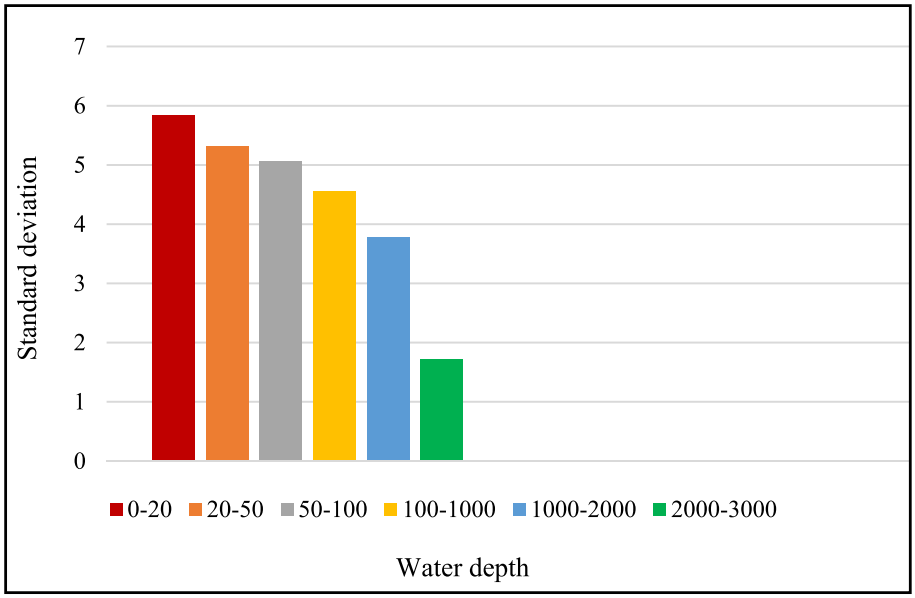

Fig. 12. The s.d. of the differences between the DTU21 and the SSv29.1 gravity models as a function of water depths.

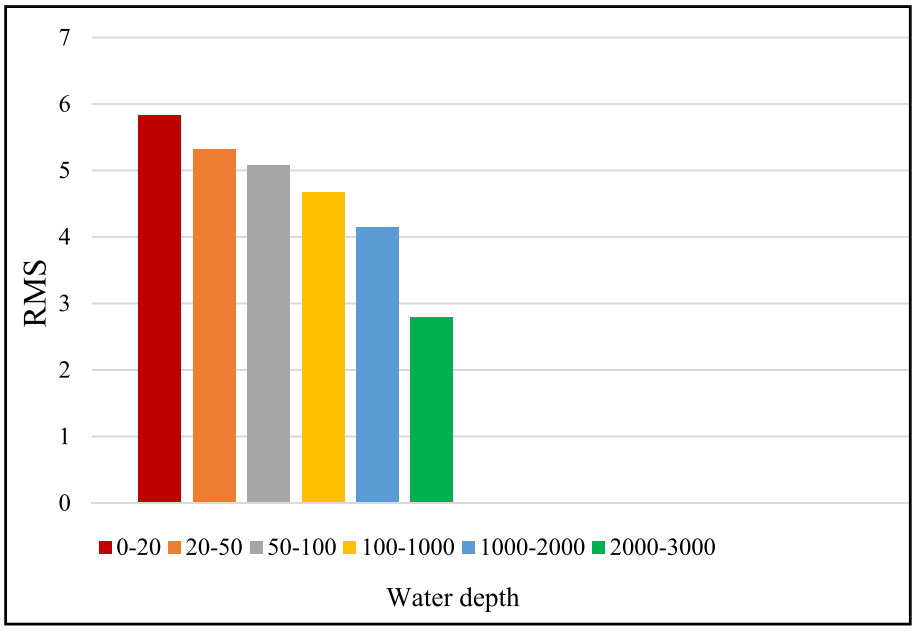

Fig. 13. The RMS of the differences between the DTU21 and the SSv29.1 gravity models as a function of water depths.

water-depth intervals are applied. The differences at a water depth range between 2000 m and 3000 m achieve the best results with a minimum, maximum, mean, s.d., and RMS of −2.18, 7.27, 2.21, 1.71, and 2.79 mGal, respectively.

Conflict of interest

All authors declare that they have no conflicts of interest.

References

Abdallah, M., Abd El Ghany, R., Rabah, M., Zaki, A., 2022. Assessments of recently released global geopotential models along the Red Sea with shipborne gravity data. Egypt. J. Remote Sens. Space Sci. 25, 125–133. https://doi.org/10.1016/j.ejrs.2022.01.005.

Andersen, O.B., Knudsen, P., 2020. The DTU17 global marine gravity field: First validation results, in: International Association of Geodesy Symposia. Springer, pp. 83–87. https://doi.org/10.1007/1345_2019_65.

Andersen, O.B., Knudsen, P., 1997. Global gravity field from the ERS-1 and the geosat geodetic mission altimetry – The Mediterranean Sea. European Space Agency, (Special Publication) ESA SP 103, 1573–1576.

Forsbergbi, R., Olesen, A.V., Alshamsi, A., Gidskehaug, A., Ses, S., Kadir, M., Peter, B., 2012. Airborne gravimetry survey for the marine area of the United Arab Emirates. Mar. Geod. 35, 221–232. https://doi.org/10.1080/01490419.2012.672874.

Li, Q., Bao, L., Wang, Y., 2021. Accuracy evaluation of altimeter-derived gravity field models in offshore and coastal regions of China. Front. Earth Sci. 9, 649. https://doi.org/10.3389/feart.2021.722019.

Liu, L., Jiang, X., Liu, S., Zheng, L., Zang, J., Zhang, X., Liu, L., 2016. Calculating the marine gravity anomaly of the south china sea based on the inverse stokes formula. IOP Conf. Ser.: Earth Environ. Sci. 46, 012062.

Pavlis, N.K., Holmes, S.A., Kenyon, S.C., Factor, J.K., 2013. Erratum: Correction to the development and evaluation of the earth gravitational model 2008 (EGM2008). J. Geophys. Res.: Solid Earth 118, 2633. https://doi.org/10.1002/jgrb.50167,2013.

Sandwell, D., Garcia, E., Soofi, K., Wessel, P., Chandler, M., Smith, W.H.F., 2013. Toward 1-mGal accuracy in global marine gravity from CryoSat-2, Envisat, and Jason-1. Leading Edge 32, 892–899. https://doi.org/10.1190/tle32080892.1.

Sandwell, D.T., Harper, H., Tozer, B., Smith, W.H.F., 2021. Gravity field recovery from geodetic altimeter missions. Adv. Space Res. 68, 1059–1072. https://doi.org/10.1016/j.asr.2019.09.011.

Sandwell, D.T., Müller, R.D., Smith, W.H.F., Garcia, E., Francis, R., 2014. New global marine gravity model from CryoSat-2 and Jason-1 reveals buried tectonic structure. Science 346 (6205), 65–67.

Sandwell, D.T., Smith, W.H.F., 2009. Global marine gravity from retracked Geosat and ERS-1 altimetry: Ridge segmentation versus spreading rate. J. Geophys. Res. Solid Earth 114, 1–18. https://doi.org/10.1029/2008JB006008.

Sandwell, D.T., Smith, W.H.F., 1997. Marine gravity anomaly from Geosat and ERS 1 satellite altimetry. J. Geophys. Res. B: Solid Earth 102, 10039–10054. https://doi.org/10.1029/96JB03223.

Wu, Y., Wang, J., Abulaitijiang, A., He, X., Luo, Z., Shi, H., Wang, H., Ding, Y., 2022. Local enhancement of marine gravity field over the spratly islands by combining satellite SAR altimeter-derived gravity data. Remote Sensing 14, 474. https://doi.org/10.3390/rs14030474.

Zaki, A., Mansi, A.H., Rabah, M., El-Fiky, G., 2018a. Validation of recently released GOCE-based satellite-only global geopotential models over the Red Sea using shipborne gravity data. Bollett. Geofisica Teorica Appl. 59, 267–284. https://doi.org/10.4430/bgta0242.

Zaki, A., Mansi, A.H., Selim, M., Rabah, M., El-Fiky, G., 2018b. Comparison of satellite altimetric gravity and global geopotential models with shipborne gravity in the Red Sea. Mar. Geod. 41, 258–269. https://doi.org/10.1080/01490419.2017.1414088.

Zhang, S., Sandwell, D.T., Jin, T., Li, D., 2017. Inversion of marine gravity anomalies over southeastern China seas from multi-satellite altimeter vertical deflections. J. Appl. Geophys. 137, 128–137. https://doi.org/10.1016/j.jappgeo.2016.12.014.